AC-Stark Shift and Dephasing of a Superconducting Qubit Strongly Coupled to a Cavity Field

D. I. Schuster, A. Wallraff, A. Blais, L. Frunzio, R.-S. Huang,* J. Majer, S. M. Girvin, and R. J. Schoelkopf Departments of Applied Physics and Physics, Yale University, New Haven, CT 06520 (Dated: February 2, 2008, submitted to PRL)

We have spectroscopically measured the energy level separation of a superconducting charge qubit coupled non-resonantly to a single mode of the electromagnetic field of a superconducting on-chip resonator. The strong coupling leads to large shifts in the energy levels of both the qubit and the resonator in this circuit quantum electrodynamics system. The dispersive shift of the resonator frequency is used to non-destructively determine the qubit state and to map out the dependence of its energy levels on the bias parameters. The measurement induces an ac-Stark shift of 0.6 MHz per photon in the qubit level separation. Fluctuations in the photon number (shot noise) induce level fluctuations in the qubit leading to dephasing which is the characteristic back-action of the measurement. A cross-over from lorentzian to gaussian line shape with increasing measurement power is observed and theoretically explained. For weak measurement a long intrinsic dephasing time of $T_2 > 200$ ns of the qubit is found.

We have recently demonstrated that a superconducting quantum two-level system can be strongly coupled to a single microwave photon [1]. The strong coupling between a quantum solid state circuit and an individual photon, analogous to atomic cavity quantum electrodynamics (CQED) [2], has previously been envisaged by many authors, see Ref. 3 and references therein. Our circuit quantum electrodynamics architecture [3], in which a superconducting charge qubit, the Cooper pair box [4], is coupled strongly to a coplanar transmission line resonator, has great prospects both for performing quantum optics experiments [5] in solids and for realizing elements for quantum information processing [6] with superconducting circuits [7].

In this letter we present spectroscopic measurements which demonstrate the non-resonant (dispersive) strong coupling between a Cooper pair box and a coherent microwave field in a high quality cavity. The quantum state of the Cooper pair box is controlled using resonant microwave radiation and is read out with a dispersive quantum non-demolition (QND) measurement [3, 8, 9]. The interaction between the Cooper pair box and the measurement field containing n photons on average gives rise to a large ac-Stark shift of the qubit energy levels, analogous to the one observed in CQED [10]. As a consequence of the strong coupling, quantum fluctuations in n induce a broadening of the transition line width, characterizing the back action of the measurement on the qubit.

In our circuit QED architecture [3], see Fig. 1a, a split Cooper pair box [4], modelled by the two-level hamiltonian $H_a = -1/2$ ($E_{\rm el} \, \sigma_x + E_{\rm J} \, \sigma_z$) [11], is coupled capacitively to the electromagnetic field of a full wave ($l = \lambda$) transmission line resonator, described by a harmonic oscillator hamiltonian $H_{\rm r} = \hbar \omega_{\rm r} (a^{\dagger} a + 1/2)$. In the Cooper pair box, the energy difference $E_a = \hbar \omega_{\rm a} = \sqrt{E_{\rm el}^2 + E_{\rm J}^2}$ between the ground state $|\downarrow\rangle$ and the first excited state $|\uparrow\rangle$, see Fig. 1b, is determined by its electrostatic energy $E_{\rm el} = 4E_{\rm C}(1 - n_{\rm g})$ and its Josephson coupling energy

 $E_{\rm J}=E_{\rm J,max}\cos{(\pi\Phi_{\rm b})}$. Here, $E_{\rm C}=e^2/2C_\Sigma\approx 5.0\,{\rm GHz}$ is the charging energy given by the total box capacitance C_Σ , $n_{\rm g}=C_g^\star V_{\rm g}/e$ is the gate charge controlled by the gate voltage V_g applied through a gate with effective capacitance C_g^\star , and $E_{\rm J,max}\approx 8.0\,{\rm GHz}$ is the maximum Josephson coupling energy of the two junctions which is modulated by applying a flux bias $\Phi_{\rm b}=\Phi/\Phi_0$ to the loop of the split box, see Fig. 1a. Near its resonance frequency $\omega_r=1/\sqrt{LC}\approx 2\pi\,6.0\,{\rm GHz}$, the resonator is accurately modelled as a harmonic oscillator with lumped inductance L and capacitance C.

In the presence of strong mutual coupling between the qubit and the resonator [1], their *dressed* excitation energies $\widetilde{\omega}_{a}$ and $\widetilde{\omega}_{r}$, are modified from their bare values ω_{a} and ω_{r} . For large detuning $\Delta_{a,r} = \omega_{a} - \omega_{r}$ the dressed energy levels are determined by the Hamiltonian [3]

$$H \approx \hbar \left(\omega_{\rm r} + \frac{g^2}{\Delta_{\rm a,r}} \sigma_z \right) a^{\dagger} a + \frac{1}{2} \hbar \left(\omega_{\rm a} + \frac{g^2}{\Delta_{\rm a,r}} \right) \sigma_z , \quad (1)$$

where $g/2\pi \approx 5.8$ MHz is the coupling strength between a single photon and the qubit [1]. In this non-resonant case, the dressed resonator frequency $\widetilde{\omega}_{\rm r} = \omega_{\rm r} \pm g^2/\Delta_{\rm a,r}$ depends on the qubit state $\sigma_z = \pm 1$ and the detuning $\Delta_{\rm a,r}$. The qubit state can thus be inferred from the phase shift ϕ that a probe microwave transmitted through the resonator at frequency $\omega_{\rm RF}$ experiences due to the interaction with the qubit [1, 3]. In Fig. 1c, the phase shift $\phi = \pm \tan^{-1}\left(2g^2/\kappa\Delta_{\rm a,r}\right)$, where $\kappa = \omega_{\rm r}/Q$ is the decay rate of photons from the resonator with quality factor $Q \approx 10^4$, is plotted versus gate charge $n_{\rm g}$. ϕ is maximum at $n_{\rm g} = 1$ where the detuning $\Delta_{\rm a,r}$ is smallest and falls off as the detuning is increased with increasing n_g . Moreover, ϕ has opposite signs in the ground $|\downarrow\rangle$ and excited $|\uparrow\rangle$ states of the CPB.

Qubit state transitions can be driven by applying an additional microwave of frequency ω_s and power P_s resonant with the qubit $(\Delta_{s,a} = \omega_s - \widetilde{\omega}_a = 0)$ to the input port of the resonator, see Fig. 1a. On resonance $(\Delta_{s,a} = 0)$

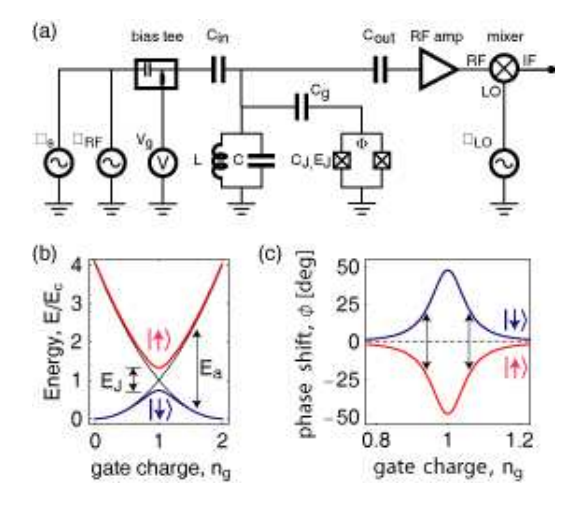


FIG. 1: (color online) (a) Simplified circuit diagram of measurement setup. The phase ϕ and amplitude T of a microwave at $\omega_{\rm RF}$ transmitted through the resonator, amplified and mixed down to an intermediate frequency $\omega_{\rm IF} = \omega_{\rm RF} - \omega_{\rm LO}$ using a local oscillator at $\omega_{\rm LO}$ is measured. An additional spectroscopy microwave at $\omega_{\rm s}$ is applied to the input port of the resonator. (b) Ground $|\downarrow\rangle$ and excited $|\uparrow\rangle$ state energy levels of CPB vs. gate charge n_g . (c) Calculated phase shift ϕ in ground and exited state vs. n_g for $\Delta_{\rm a,r}/2\pi=100\,{\rm MHz}.$

and for a continuous (cw) large amplitude spectroscopy drive, the qubit transition saturates and the population in the exited and ground state approaches 1/2. In this case, the measured phase shift of the probe beam at $\omega_{\rm RF}$ is expected to saturate at $\phi = 0$, see Fig. 1c. By sweeping the spectroscopy frequency $\omega_{\rm s}$ vs. the gate charge $n_{\rm g}$ and continuously measuring ϕ we have mapped out the energy level separation $\widetilde{\omega}_a$ of the qubit, see Fig. 2. In the lower panel of Fig. 2a, the measured phase shift ϕ is shown for the non-resonant case, where $\omega_{\rm s} < \widetilde{\omega}_{\rm a}$ for all values of gate charge $n_{\rm g}$. The measured phase shift is, as expected, a continuous curve similar to the one shown in Fig. 1c. In the middle panel of Fig. 2a, the spectroscopy microwave at $\nu_{\rm s} = \omega_{\rm s}/2\pi = 6.15\,{\rm GHz}$ is in resonance with the qubit at $n_{\rm g} = 1$, populating the excited state and thus inducing a dip in the measured phase shift ϕ around $n_{\rm g} = 1$, as expected. Note that, as predicted [3], our measurement scheme has the advantage of being most sensitive at charge degeneracy, a bias point where traditional electrometry, using a radio frequency single electron transistor (rf-SET) [12] for example, is unable to distinguish the qubit states.

When $\nu_{\rm s}$ is increased to higher values, resonance with the qubit occurs for two values of $n_{\rm g}$ situated symmetrically around $n_{\rm g}=1$, leading to two symmetric dips in ϕ , see upper panel of Fig. 2a. From the $[n_g,\nu_s]$ positions of the spectroscopic lines in the measured phase ϕ , the Josephson energy $E_{\rm J}=6.2\,{\rm GHz}$ and the charging energy $E_{\rm C}=4.8\,{\rm GHz}$ are determined in a fit using the full qubit Hamiltonian [11], see density plot of ϕ vs. $n_{\rm g}$

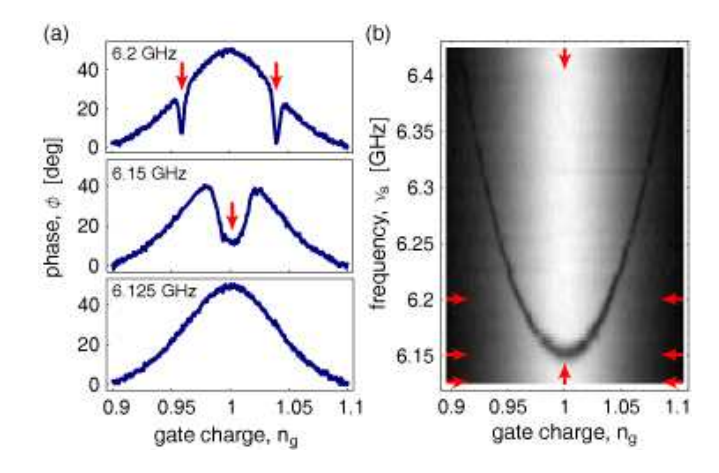


FIG. 2: (color online) (a) Probe microwave phase shift ϕ vs. gate charge $n_{\rm g}$ at spectroscopy frequency $\nu_{\rm s}=6.125\,{\rm GHz}$ (lower panel), 6.15 GHz (middle panel) and 6.2 GHz (upper panel). (b) Density plot of ϕ vs. $n_{\rm g}$ and $\nu_{\rm s}$, white (black) corresponds to large (small) phase shift. Horizontal arrows indicate line cuts shown in (a), vertical arrows indicate line cuts shown in Fig. 3a.

and ν_s in Fig. 2b. In this experiment the flux bias Φ_b has been chosen to result in a minimum detuning of about $\Delta_{\rm r,a}/2\pi \approx 100\,{\rm MHz}$ at $n_{\rm g}=1$. The tunability of $E_{\rm J}$ (i.e. the detuning at charge degeneracy) has been demonstrated previously [1]. It is also worth noting, that the spectroscopy frequency $\omega_{\rm s}$ typically remains strongly detuned ($\Delta_{\rm s,r}=\omega_{\rm s}-\omega_{\rm r}>2\pi\,100\,{\rm MHz}$) from the resonator, such that a large fraction of the spectroscopy photons are reflected at the input port and only a small number n_s , determined by the lorentzian line shape of the resonator, populates the resonator.

Various other radio or microwave frequency qubit readout schemes have been developed recently [12, 13, 14]. In particular in a closely related experiment, the level separation of a split Cooper pair box coupled *inductively* to a *low frequency, moderate Q* tank circuit has been determined spectroscopically [15].

The width and the saturation level of the spectroscopic lines discussed above depend sensitively on the power $P_{\rm s}$ of the spectroscopic drive. Both quantities can be extracted from the excited state population

$$P_{\uparrow} = 1 - P_{\downarrow} = \frac{1}{2} \frac{n_s \omega_{\text{vac}}^2 T_1 T_2}{1 + (T_2 \Delta_{\text{s},01})^2 + n_s \omega_{\text{vac}}^2 T_1 T_2}, \quad (2)$$

found from the Bloch equations in steady state [16], where $\omega_{\rm vac}=2g$ is the vacuum Rabi frequency, n_s the average number of spectroscopy photons in the resonator, T_1 the relaxation time and T_2 the dephasing time of the qubit. We have extracted the transition line width and saturation from spectroscopy frequency scans for different drive powers $P_{\rm s}$ with the qubit biased at charge degeneracy ($n_{\rm g}=1$). We observe that the spectroscopic lines have a lorentzian line shape, see Fig. 3a, with width

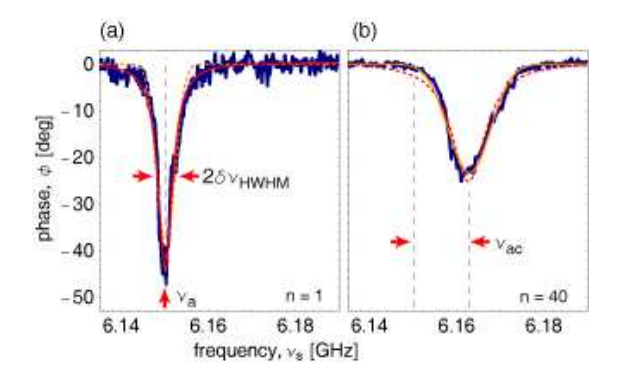


FIG. 3: (color online) Measured spectroscopic lines (blue lines) at (a) intra resonator photon number $n\approx 1$ ($P_{\rm RF}=-30\,{\rm dBm}$) with fit to lorentzian line shape (solid line) and at (b) $n\approx 40$ ($P_{\rm RF}=-16\,{\rm dBm}$) with fit to gaussian line shape (solid line). Dashed lines are best fits to (a) gaussian or (b) lorentzian line shapes, respectively. The qubit transition frequency $\nu_{\rm a}$ at low $P_{\rm RF}$, the half width half max $\delta\nu_{\rm HWHM}$ and the ac-Stark shift $\nu_{\rm ac}$ of the lines are indicated.

and depth in accordance with Eq. (2). The half width at half max (HWHM) of the line is shown to follow the expected power dependence $2\pi\delta\nu_{\rm HWHM} = 1/T_2' =$ $\sqrt{1/T_2^2 + n_s \omega_{\rm vac}^2 T_1/T_2}$ [16], where the input microwave power P_s is proportional to $n_s\omega_{\rm vac}^2$, see Fig. 4a. In the low power limit $(n_s\omega_{\rm vac}^2\to 0)$, the unbroadened line width is found to be small $\delta \nu_{\rm HWHM} \approx 750\,{\rm kHz}$, corresponding to a long dephasing time of $T_2 > 200\,\mathrm{ns}$ at $n_\mathrm{g} = 1$, where the qubit is maximally protected from 1/f charge fluctuations. At larger drive, the width increases proportionally to the drive amplitude. The depth of the spectroscopic dip at resonance ($\Delta_{s,a} = 0$) reflects the probability of the qubit to be in the excited state P_{\uparrow} and depends on P_s as predicted by Eq. (2), see Fig. 4b. At low drive the population increases linearly with $P_{\rm s}$ and then approaches 0.5 for large $P_{\rm s}$.

In the above we have demonstrated that the strong coupling of the qubit to the radiation field modifies the resonator transition frequency in a way that can be exploited to measure the qubit state. Correspondingly, the resonator acts back onto the qubit through their mutual strong coupling. Regrouping the terms of the hamiltonian in Eq. (1) one sees that the dressed qubit level separation is given by $\widetilde{\omega}_a = \omega_a + 2ng^2/\Delta_{a,r} + g^2/\Delta_{a,r}$, where we note that the resonator gives rise to an ac-Stark shift of $\pm ng^2/\Delta_{\rm a,r}$, proportional to the intra-resonator photon number $n = \langle a^{\dagger}a \rangle$, as well as a Lamb shift $\pm g^2/2\Delta_{a.r.}$ due to the coupling to the vacuum fluctuations, of the qubit levels. The ac-Stark shift is observed in a measurement in which we perform spectroscopy at $n_{\rm g}=1$ for fixed spectroscopy power $P_{\rm s}$ and vary the probe beam power P_{RF} , to change the average number n of measurement photons in the resonator, see Fig. 5a. As expected, it is observed that the qubit level separation $\tilde{\nu}_{\rm a} = \tilde{\omega}_{\rm a}/2\pi$ is linear in $P_{\rm RF}$, i.e. the ac-Stark shift $\nu_{\rm ac} = 2ng^2/2\pi\Delta_{\rm a,r}$

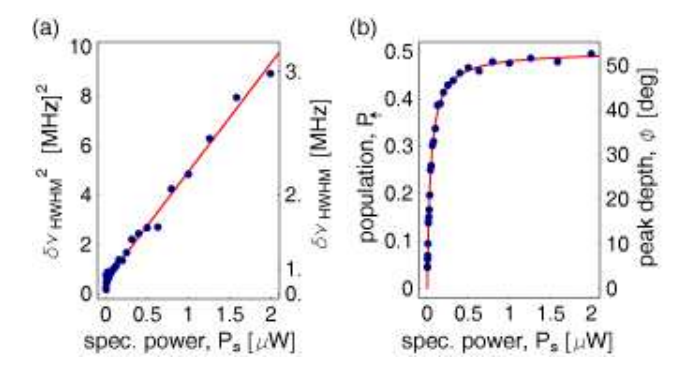


FIG. 4: (color online) (a) Measured qubit line width $\delta\nu_{\rm HWHM}$ vs. input spectroscopy power $P_{\rm s}$ (solid circles) with fit (solid line). Probe beam power $P_{\rm RF}$ is adjusted such that n<1. (b) Measured peak depth ϕ and excited state population probability P_{\uparrow} on resonance $\Delta_{\rm s,01}=0$ vs. $P_{\rm s}$ (solid circles) with fit (solid line).

being linear in the photon number n is observed. In the limit of $P_{\rm RF} \to 0 \ (n \to 0)$, the bare qubit level separation $\omega_{\rm a} + g^2/\Delta_{\rm a,r} = 2\pi \, 6.15 \, {\rm GHz}$ is determined, where $g^2/\Delta_{\rm a,r}$ is the small Lamb shift which can not be separated from $\omega_{\rm a}$ in our current experiments. Knowing the coupling constant q from an independent measurement of the vacuum Rabi mode splitting [1] and having determined $\Delta_{a,r}$ from spectroscopic measurements in the $n \to 0$ limit, the dependence of the intra-resonator photon number n on the input power P_{RF} is determined from the measured ac-Stark shift ν_{ac} . We find that an input microwave power of $P_{\rm RF} = -31 \, {\rm dBm}$ corresponds to n = 1 which is consistent with an intended attenuation of approximately 105 dB in the input coaxial line. The ac-Stark shift of the qubit at this particular detuning is a remarkable 0.6 MHz per photon in the cavity and is comparable to the line width. Using this method, the intra-resonator photon number was accurately calibrated for the vacuum Rabi mode splitting measurements presented in Ref. 1.

Quantum fluctuations (photon shot noise) δn around the average photon number n of the coherent field populating the resonator give rise to random fluctuations in the qubit transition frequency due to the ac-Stark shift. This leads to measurement induced dephasing, and thus, to a broadening of the qubit line width, see Figs. 3 and 5. This is the measurement back action and can be understood quantitatively by considering the relative phase $\varphi(t) = 2g^2/\Delta_{\rm a,r} \int_0^t dt' \delta n(t')$ accumulated in time between the ground and excited state of the qubit. Following Ref. 3, the measurement-induced phase decay of the qubit is then characterized by

$$\langle e^{i\varphi(t)}\rangle = \exp\left[-\frac{2g^4}{\Delta_{\text{a,r}}^2} \iint_0^t dt_1 dt_2 \langle \delta n(t_1)\delta n(t_2)\rangle\right]$$
 (3)

where the fluctuations δn are assumed to be gaussian. In the above expression, the photon correlation function $\langle \delta n(t) \delta n(0) \rangle = n \exp(-\kappa |t|/2)$ of the coherent probe

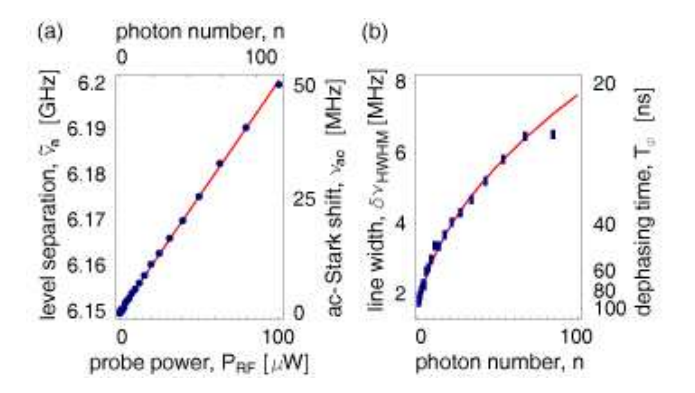


FIG. 5: (color online) (a) Measured qubit level separation $\tilde{\nu}_{\rm a}$ and fit (solid line) vs. input microwave probe power $P_{\rm RF}$. The ac-stark shift $\nu_{\rm ac}$ and the intra-resonator photon number n extracted from the fit are also indicated. (b) Measurement broadened qubit line width $\delta\nu_{\rm HWHM}$ vs. n. The corresponding total dephasing time $T_{\varphi}=1/2\pi\delta\nu_{\rm HWHM}$ as reduced by the measurement is also indicated. The fit (solid line) is obtained from Eq. (4) with a spectroscopy power broadened $T_2'\approx 105\,\rm ns.$

beam in the resonator is governed by the cavity decay rate κ and physically represents the white photon shot noise filtered by the cavity response. The spectroscopic line shape $S(\omega)$ is obtained from the Fourier transform of $\langle \exp[i\varphi(t)]\rangle e^{-t/T_2'}$ where $1/T_2'$ takes into account dephasing mechanisms independent of the measurement

$$S(\omega) = \frac{1}{\pi} \sum_{j=0}^{\infty} \frac{(-4\chi)^j}{j!} \frac{1/T_2' + 2\kappa\chi + j\kappa/2}{(\omega - \tilde{\omega}_a)^2 + \left(\frac{1}{T_2'} + 2\kappa\chi + \frac{j\kappa}{2}\right)^2}.$$
(4)

The form of the line shape depends on the dimensionless parameter $\chi = n\theta_0^2$ where $\theta_0 = 2g^2/\kappa\Delta_{\rm a,r}$ is the transmission phase shift describing the strength of the measurement. For small χ the measurement rate is slow compared to κ and the phase diffuses in a random walk $\langle \varphi(t)^2 \rangle \sim 4\theta_0^2 n\kappa t$ leading to a homogeneously broadened lorentzian line of HWHM of $2\theta_0^2 n\kappa + 1/T_2'$. For large χ , i.e. strong measurement, the measurement rate exceeds κ leading to a qubit transition frequency which depends on the instantaneous value of the cavity photon number and hence an inhomogeneously broadened gaussian line, see Fig. 3b, whose variance is simply \sqrt{n} multiplied by the Stark shift per photon. The full cross-over from intrinsic lorentzian lineshape with width $\propto n$ at small n to gaussian lineshape with width $\propto \sqrt{n}$ at large n as described by Eq. (4) is in excellent agreement with the measured dependence of the line width on n, see Fig. 5b.

In our experiments we have demonstrated that the strong coupling of a Cooper pair box to a non-resonant microwave field in a on-chip cavity gives rise to a large qubit dependent shift in the excitation energy of the resonator. This is used to perform a QND measurement of the qubit. In the qubit, the ac-Stark effect shifts the

qubit level separation by about one line width per photon and the back-action of the fluctuations in the field gives rise to a large broadening of the qubit line.

We would like to thank Michel Devoret for numerous discussions. This work was supported in part by the National Security Agency (NSA) and Advanced Research and Development Activity (ARDA) under Army Research Office (ARO) contract number DAAD19-02-1-0045, the NSF ITR program under grant number DMR-0325580, the NSF under grant number DMR-0342157, the David and Lucile Packard Foundation, the W. M. Keck Foundation, and the Natural Science and Engineering Research Council of Canda (NSERC).

- * Department of Physics, Indiana University, Bloomington, IN 47405
- [1] A. Wallraff, D. Schuster, A. Blais, L. Frunzio, R.-S. Huang, J. Majer, S. Kumar, S. Grivin, and R. Schoelkopf, Nature (London) vol, page (2004), (in press, also: cond-mat/0407325).
- H. Mabuchi and A. Doherty, Science 298, 1372 (2002).
- [3] A. Blais, R.-S. Huang, A. Wallraff, S. Girvin, and R. Schoelkopf, Phys. Rev. A 69, 062320 (2004).
- [4] V. Bouchiat, D. Vion, P. Joyez, D. Esteve, and M. H. Devoret, Physica Scripta T76, 165 (1998).
- [5] D. Walls and G. Milburn, Quantum optics (Spinger-Verlag, Berlin, 1994).
- [6] M. A. Nielsen and I. L. Chuang, Quantum computation and quantum information (Cambridge University Press, 2000).
- [7] Y. Nakamura, Y. A. Pashkin, and J. S. Tsai, Nature 398, 786 (1999). D. Vion et al., Science 296, 886 (2002).
 J. M. Martinis, S. Nam, J. Aumentado, and C. Urbina, Phys. Rev. Lett. 89, 117901 (2002). Y. Yu et al., Science 296, 889 (2002). I. Chiorescu, Y. Nakmura, C. J. P. M. Harmans, and J. E. Mooij, Science 299, 1869 (2003). T. Yamamoto et al., Nature 425, 941 (2003).
- [8] P. Grangier, J. A. Levenson, and J.-P. Poziat, Nature (London) 396, 537 (1998).
- [9] G. Nogues, A. Rauschenbeutel, S. Osnaghi, M. Brune, J. M. Raimond, and S. Haroche, Nature (London) 400, 239 (1999).
- [10] P. Brune, M. Nussenzweig, F. Schmidt-Kaler, F. Bernadot, A. Maali, J. M. Raimond, and S. Haroche, Phys. Rev. Lett. 72, 3339 (1994).
- [11] Y. Makhlin, G. Schön, and A. Shnirman, Rev. Mod. Phys. 73, 357 (2001).
- [12] K. Lehnert, K. Bladh, L. Spietz, D. Gunnarsson, D. Schuster, P. Delsing, and R. Schoelkopf, Phys. Rev. Lett. 90, 027002 (2003).
- [13] A. Lupascu, C. J. M. Verwijs, R. N. Schouten, C. J. P. M. Harmans, and J. E. Mooij (2003), cond-mat/0311510.
- [14] I. Siddiqi, R. Vijay, F. Pierre, C. Wilson, M. Metcalfe, C. Rigetti, L. Frunzio, and M. H. Devoret (2003), condmat/0312623.
- [15] D. Born, V. I. Shnyrkov, W. Krech, T. Wagner, E. Il'ichev, U. Hübner, and H.-G. Meyer (2003), condmat/0312696.
- [16] A. Abragam, The principles of nuclear magnetism (Oxford University Press, 1961).